

Compression and Escape of Copolymers of Adsorbing and Nonadsorbing Blocks

J. Ennis*[†] and E. M. Sevick

Research School of Chemistry, Australian National University, Canberra, ACT 0200, Australia

Received May 22, 2000; Revised Manuscript Received November 27, 2000

ABSTRACT: We describe the escape transition of a block copolymer chain compressed between finite-sized obstacles. Two different and independent theoretical methods are used, and both provide a similar description of multiple escape transitions where the number and critical compression are determined by the sizes and ordering of the blocks. We predict that the compressive force profile could have a specific “signature” of transitions which would give information about the polymer architecture.

1. Introduction

The problem of a polymer confined within a narrow slit is a classic problem that is generally well understood.^{1,2} More recently, researchers have explored a related problem: a chain end-tethered to a surface and compressed by an obstacle, say the flat end of a cylinder, whose size is not much larger than the natural dimension of the chain.^{3–13} When compressed weakly, the chain does not “see” the edge of the compressing obstacle, it deforms uniformly, and the force that the chain imposes on the obstacle grows monotonically with compression. However, beyond a critical compression, the chain can reduce its energy by forming a stretched umbilical tether from the grafting point to the edge of the disk so that many of the monomers in the chain can “escape” from underneath the compressing obstacle. Upon such escape, the compressive force decreases abruptly, signaling the reduction in the number of monomers trapped beneath the cylindrical obstacle. Depending upon the diameter of the compressing cylinder relative to the natural size of the chain, there can be a significant energetic barrier to escape associated with the extra energy that is needed to stretch the chain to the edge of the obstacle. In this case, the escape transition can be described as a first-order transition between “states” of a chain: imprisoned and escaped. This escape transition has been described using theory and computer simulation, and a recent series of papers have investigated the sharpness of this escape transition.^{10,11,13} The simple mean-field treatments predict a sharp, discontinuous drop in the compressive force at or near the transition. Several simulations confirm the existence of this transition; however, thermal fluctuations can “blur” the sharpness of the transition. An exact calculation of the partition function of an ideal chain shows unambiguously that the escape transition occurs and is marked by a maximum and minimum in the force profile. This escape transition has not been observed experimentally, but it should be possible to investigate this by compressing a surface-tethered chain with the polished tip of an atomic force microscope (AFM).

[†] Current address: CSIRO Petroleum, P.O. Box 3000, Glen Waverley VIC 3150, Australia.

* Corresponding author. E-mail: j.ennis-king@dpr.csiro.au.

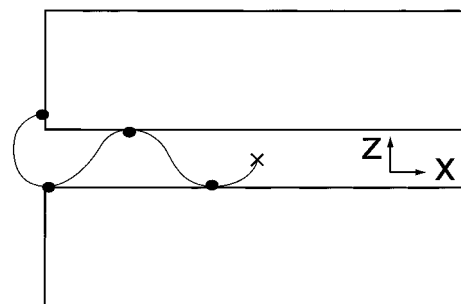


Figure 1. Schematic of the compression of a multiblock copolymer end-tethered between the flat ends of two cylinders. The chain consists of alternating blocks of adsorbing stickers (which are laterally mobile) and nonadsorbing blocks with one end permanently fixed at the radial center and midpoint between the faces of the cylinder. The compression distance, H , is the size of the gap between the cylinders, and L is the radius of the cylinders. A chain is wholly confined if all monomers are confined within the gap and between the flat ends of the cylinders. The first escape transition occurs when compression leads to the partial expulsion of the chain from between the cylinder faces. Subsequent escape transitions can occur at higher compressions (or smaller H) where there is a sudden further expulsion of monomers.

We investigate the compression of a block copolymer comprised of adsorbing blocks, distributed along the linear backbone of an otherwise nonadsorbing chain. Such a block copolymer can exhibit multiple escape transitions. These additional escape transitions occur as successive blocks or groups of contiguous blocks are “squeezed out” from underneath the confining obstacle. As a result of the dramatically reduced number of monomers, the force required to compress the chain between two finite-sized obstacles can exhibit several maxima, and the number of these depends on the size, number, and ordering of the blocks along the chain contour. That is, the compressive force profiles are sensitive to the architecture of the chain.¹⁴ The linear chains considered here are comprised of alternating blocks of adsorbing monomers and nonadsorbing monomers with one end permanently fixed at the radial center and midpoint in the gap between the flat ends of two cylinders of radius L (Figure 1). The width of the gap, H , is a controlled distance and is referred to as the compression distance: H is small when the system is strongly compressed and is large when the system is

weakly compressed. For simplicity and theoretical tractability in this treatment, ideal chains are employed; i.e., even though monomers are excluded from the obstacles and may be attracted to the obstacle surfaces, there are no interactions between the monomers. We focus upon the case where all surfaces, that is the faces of the opposing cylinders and their sides, are equally attractive to the adsorbing monomers, although one of the approaches that we use allows for different adsorption strengths on the faces and on the sides.

In this paper we present calculations of the force profile (and other quantities) that demonstrate the multiple transitions that can occur for block copolymers. Two different and independent theoretical methods are employed in this paper. The first method, described in the following section, is an approximate state model for long chains where we express the free energy of the chain in various "states", each of which is characterized by the number of escaped blocks. The conformational entropy of a chain is usually approximated by the known result for a polymer confined in an infinite slit; however, we show that incorporation of the loop structure of nonadsorbing blocks in the entropy description leads to multiple escape transitions. This simple model provides a simple physical picture of multiple escape transitions for the case of strongly adsorbing monomers. The second and more rigorous approach is described in sections 3 and 4 and consists of numerically evaluating the partition function of a finite-sized chain underneath finite-sized obstacles. This approach allows for monomers that adsorb with an adjustable adsorption strength; however, we focus mainly upon the case of strongly adsorbing blocks for comparison with the simple model of section 2. This calculation is limited only by the numerical precision of the computer and allows us to study the escape transitions for finite sizes via a procedure that is essentially exact. This and the approximate state model show similar results: the sizes and ordering of blocks along the chain contour determine the number of escape transitions and the critical compressions at which they occur.

2. An Approximate State Model

A simple state model that was used to first describe the escape transition of an ideal end-tethered homopolymer under a finite obstacle^{6,13} is an instructive starting point. This approach consists of writing down approximate expressions for the energy of confinement of the polymer trapped beneath an obstacle and for the stretching energy associated with the umbilical tether of a partially escaped chain. The entropic penalty of confinement of the chain promotes escape while the stretching penalty required for the formation of the umbilical tether suppresses escape: a balance of these energies predicts a critical compression at which the chain first escapes. We can review this model in terms of a compressed block copolymer whose nonadsorbing blocks are ideal and are separated by adsorbing blocks that are taken to be "sticky" points along the chain contour. These sticky points are sufficiently strongly adsorbing that they are always located at the surface of the obstacle but are otherwise laterally mobile. Let m be the number of nonadsorbing blocks and denote by n_i the number of monomers in block i , where the index $i = 1$ labels the block nearest the tethered end of the chain. The total number of monomers is $N = \sum_{i=1}^m n_i$, and the contribution of the i th nonadsorbing block to

the chain is given by the fraction $r_i = n_i/N$. The dimensionless compression distance is defined as $\tilde{H} = H/R_g$, and the dimensionless obstacle radius is $\tilde{L} = L/R_g$.

In this simple first-order approach, the entropic penalty for confinement of block i between surfaces separated by H is approximated by $k_B T \pi^2 r_i / \tilde{H}^2$ where $a \ll H < R_g$ and a is the monomer size. This approximate entropic penalty can be simply constructed by counting the number of times that we expect a chain confined in an infinite slit of height H to intersect the walls and multiplying by the entropy lost upon chain reflection from the wall, $\approx k_B T$.¹⁵ It is important to note that this is the leading term in the free energy of an ideal chain of n_i monomers in an infinite slit.^{16,17} Since this is linear in n_i , it follows that to first order the free energy of a fully confined block copolymer depends on the total number of monomers in these blocks and not upon the distribution of block sizes. Thus, if part of the chain escapes such that there are only p monomers or $r = p/N$ of the chain remaining in the slit, then the confinement penalty is approximately $k_B T \pi^2 r / \tilde{H}^2$ irrespective of how those p monomers are distributed within blocks.

The energy penalty associated with stretching a chain tether from its tethering point to the edge of the obstacle is approximated as $k_B T \tilde{L}^2 / (4r)$. Thus, at any compression, \tilde{H} , if the chain is fully confined, then its free energy is comprised of simply the confinement penalty, $k_B T \pi^2 / \tilde{H}^2$. If the chain has partly escaped, then the free energy is given by the sum of the penalty of partial confinement and the stretching penalty, $k_B T (\pi^2 r^* / \tilde{H}^2 + \tilde{L}^2 / (4r^*))$ where r^* is that value which minimizes the energy. The minimum free energy of the escaped state is $k_B T \pi \tilde{L} / \tilde{H}$, which occurs when $r^* = \tilde{L} \tilde{H} / (2\pi)$. Comparing this to the free energy of the fully confined state, and adopting the lowest energy configuration as representative of the state of the chain, it can be shown that the escape of the chain first occurs at $\tilde{H} = \pi / \tilde{L}$ when $r = 1/2$ or when the fraction of nonadsorbing monomers that have escaped jumps from zero to one-half. The maximum force f on the chain just before escape can be computed by taking the derivative of the free energy with respect to separation and is given by $f R_g / (k_B T) = 2 \tilde{L}^3 / \pi$.

This first-order treatment predicts that the block copolymer behaves under compression in the same manner as a nonadsorbing homopolymer with the same number of monomers, i.e., with a single escape transition upon compression. Before refining the approximate energy expressions, we should note how well these expressions describe the escape of an end-tethered homopolymer. In an earlier paper,¹³ we solved the partition function for the case of a nonadsorbing homopolymer chain of finite length compressed between two cylinders. Effectively, this is an exact calculation with full enumeration of the chain's conformations. By careful extrapolation of those numerical results to the long chain limit, we find that the rigorous treatment predicts an escape transition at $\tilde{H} \tilde{L} = 3.0 \pm 0.1$ and $f \tilde{L}^3 R_g / (k_B T) = 0.65 \pm 0.03$. These estimates agree well with the approximate state model above, which gives values of π and $2/\pi$, respectively. However, as we will show in the following section of this paper, an exact solution of the block copolymer case provides multiple or secondary escape transitions commensurate with the block structure of the polymer. We are able to capture these secondary transitions in an approximate way

by accounting for the entropic confinement penalty of loops.

It is convenient to work with free energy expressions for various possible states where the conformational entropy term is cast in its most general terms. Let $g(\tilde{H}/r)$ denote the entropic penalty for confinement of a block of rN nonadsorbing monomers in an infinite slit of separation H . Then the Helmholtz free energy of a wholly confined block copolymer is

$$F_m = \sum_{i=1}^m g\left(\frac{\tilde{H}}{r_i}\right) \quad (1)$$

Let us define the j th state as an ensemble of chains with the following configuration: the first j nonadsorbing blocks are fully confined, at least part of the $j+1$ st block has escaped, and the remaining $j+2$ through m blocks are wholly escaped. The Helmholtz free energy of the j th state is denoted by F_j and for $0 \leq j \leq m-1$ is

$$F_j = \sum_{i=1}^j g\left(\frac{\tilde{H}}{r_i}\right) + g\left(\frac{\tilde{H}}{r^*}\right) + \frac{\tilde{L}^2}{4(\sum_{i=1}^j r_i + r^*)} \quad (2)$$

where r^* is that value which minimizes F_j and satisfies $0 < r^* < r_{j+1}$. The first sum on the right-hand side is the entropic penalty of the blocks that are fully confined between the obstacles, while the next term is the confinement penalty of the partially confined block, and the last term is the energy required to stretch the confined part of the chain from the tethering point to the edge of the slit. The chain can readjust the number of monomers in block $j+1$ that remain confined between the obstacles so as to minimize the free energy. As in the first-order approximation, the free energy of the escaped part of the chain is ignored, since this is relatively small compared to the contributions from the confined part of the chain.

At any given separation, the state of the chain, i.e., whether it is fully confined or in one of several partially escaped j states, can now be predicted in one of two ways. The first way is to assume that the chain resides in the state of lowest free energy, denoted F_{\min} . This is reasonable when the energy differences between states are large compared to the thermal energy $k_B T$ such that fluctuations between states can be safely ignored. The compressive force f on the chain is then given by $fR_g/(k_B T) = -\partial F_{\min}/\partial \tilde{H}/(k_B T)$. The second way is to approximate the partition function by

$$Q = \sum_{j=0}^m \exp(-F_j/(k_B T)) \quad (3)$$

so that the free energy is given by $-k_B T \ln Q$. This approach ignores prefactors that relate to the occupancy of the different states but accounts for some fluctuations between the states. Then the force f on the chain is calculated from $fR_g/(k_B T) = 1/Q \partial Q/\partial \tilde{H}$.

To complete the calculation, it is necessary to specify $g(\tilde{H})$, the conformational entropy of a block confined in an infinite slit. A block of nonadsorbing monomers is topologically equivalent to a loop as the ends of the block stick to surfaces. Using the approach of Dolan and Edwards,^{13,16} one can show that to within an additive

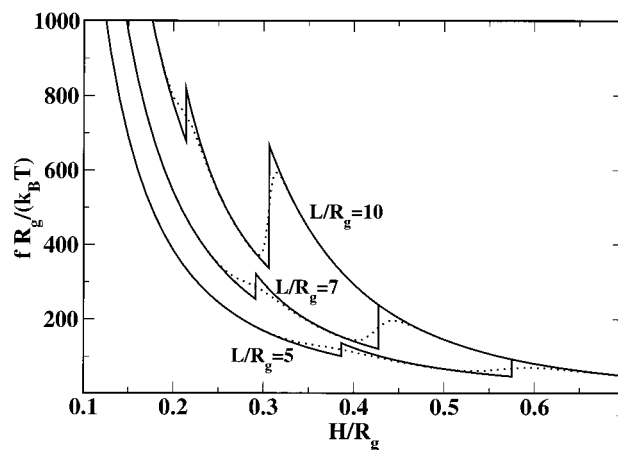


Figure 2. Dimensionless force, $fR_g/(k_B T)$, vs dimensionless compression distance, \tilde{H} , for a chain consisting of two nonadsorbing blocks separated by sticky point blocks, as predicted by the state model where higher-order terms are included in the calculation of the conformational entropy. The results are plotted for three different obstacle sizes, \tilde{L} , where the ratio of the first block (nearest the tethering point) to the second nonadsorbing block is fixed at 3:2. Results are given in two approximate cases. In the first case, fluctuations between states are disallowed, and the conformational state of the chain is that state of lowest Helmholtz free energy (solid lines) and results in discontinuous compressive force at escape transitions. In the second case (dotted lines), fluctuations between states are allowed and approximated by an unweighted mixing of states in the partition function, eq 3. This leads to a “blurring” of the force jumps.

constant the confinement penalty of a loop is

$$g(\tilde{H}) = -k_B T \ln \left(\frac{4\pi^{5/2}}{\tilde{H}^3} \sum_{n=1}^{\infty} n^2 \exp\left(-\frac{\pi^2 n^2}{\tilde{H}^2}\right) \right) \quad (4)$$

At large separations ($\tilde{H} \gg 1$) a useful alternative form that converges more quickly is

$$g(\tilde{H}) = -k_B T \ln \left(1 + 2 \sum_{n=1}^{\infty} \exp(-n^2 \tilde{H}^2) (1 - 2n^2 \tilde{H}^2) \right) \quad (5)$$

If one uses only the leading term of eq 4 at small separations, so that $g(\tilde{H}) \approx k_B T \pi^2 / \tilde{H}^2$, then one recovers the first-order scaling analysis described at the start of this section. This yields the simple, single escape transition at $r = 1/2$ that has been described for homopolymers. If further terms in $g(\tilde{H})$ are included in the analysis, then in some cases additional escape transitions are predicted to occur. We retain terms up to $n = 5$ in the numerical calculations, although essentially the same results are obtained with only one or two extra terms. We have assumed that the entropy associated with the sticky points along the chain is unchanged as these remain at the surface (while still being laterally mobile) irrespective of whether the chain is confined or escaped. This assumption of strongly binding stickers can be relaxed in the exact calculations in the next section, allowing the sticky monomers to desorb from the surface.

Figure 2 is the compressive force profile for three different sized obstacles as predicted from the state model with the confinement penalty calculated for loops. The chain is comprised of two nonadsorbing blocks; the first (nearest the tethering point) has 0.4 N monomers, while the second block has 0.6 N monomers. If the state

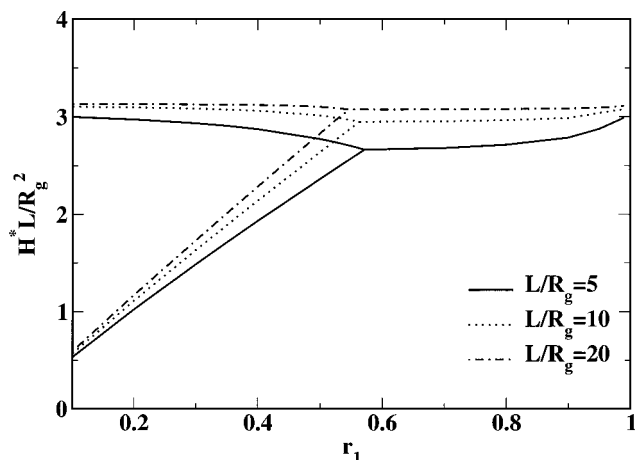


Figure 3. Locus of critical compressions at which escape transitions occur for a copolymer with two nonadsorbing blocks separated by a short sticky block as a function of the size of the first nonadsorbing block (located closest to the tethering point). The critical compression is expressed as $\tilde{H}^* \tilde{L}$ where \tilde{L} is the fixed size of the obstacle. The size of the first block is expressed as the fractional contour of the chain or $r_1 = n_1/N$ where n_1 is the number of monomers in the first block and N is the total number of monomers. These predictions are a result of the approximate state model where higher-order terms are included in the calculation of the conformation entropy and where the state of the chain is determined by that of lowest free energy.

of the chain is chosen as that of lowest free energy, then the resulting force curves are the solid lines. For this chain architecture there are two discontinuous escape transitions that occur at smaller separations as the obstacle size increases. The first transition which occurs at the weaker compression corresponds to the chain first escaping from between the cylinders, and the second transition occurs as the number of monomers confined between the cylinders is reduced discontinuously. Each escape transition corresponds to the escape of a block. Compressive force profiles that are calculated from the approximate partition function, eq 3, are given by the dotted lines. The first escape transition is “blurred” but still distinguishable as a local maximum and minimum in the force curve. But the second escape transition becomes an inflection rather than a local maximum. This may be due to the probably inappropriate weighting in the approximate partition function. As we will show in the following sections, secondary transitions are also evident from the more rigorous partition function calculations.

The number of escape transitions predicted for a polymer with two nonadsorbing blocks should depend on the relative sizes of the blocks. Figure 3 shows the locus of critical compression distances H^* at which escape transitions occur as the size of the first block, $r_1 = n_1/N$, is varied. The results are plotted as a dimensionless critical compression, $\tilde{H}^* \tilde{L}$, demonstrating that as \tilde{L} increases from 5 to 20, the critical compressions \tilde{H}^* scale roughly as \tilde{L}^{-1} . That is, escape occurs at more severe compression (i.e., smaller separations) for larger obstacle sizes. A vertical trace on this figure corresponds to a compression experiment where the separation is lowered from $\tilde{H} \tilde{L}$ toward zero. At large separations, $\tilde{H} \tilde{L} > 3.0$, the entire block copolymer is confined between the obstacles, and as we compress, portions of the chain discontinuously escape at $\tilde{H}^* \tilde{L}$ where the vertical trace intersects the loci of critical compression distances. There is clearly a maximum size of the first block $r_1 \approx$

0.5–0.6, below which two escape transitions occur and above which only one transition occurs, and this maximum block size depends weakly on the obstacle size \tilde{L} .

The compression at which the first escape transition occurs (i.e., the one which occurs at largest separation or weakest compression) is relatively constant as r_1 changes, particularly for large obstacles (i.e., large \tilde{L}). This suggests the following picture. For large obstacles where smaller separations are required in order to see an escape transition, $g(\tilde{H})$ is well-approximated by the leading term $k_B T \pi^2 / \tilde{H}^2$. Consequently, the first escape transition occurs at compressions similar to that of a nonadsorbing homopolymer irrespective of the size of the first block. That is, escape occurs at $\tilde{H} \tilde{L} \approx 3.0$ with half of the monomers escaping. Note that for $\tilde{L} = 20$ our results show that the first escape transition occurs at $\tilde{H} \tilde{L} \approx 3.0$ and is almost independent of the first block size, r_1 . If $r_1 > 0.5$, then this first escape causes the escape of the “sticker” block that divides the two nonadsorbing blocks such that both nonadsorbing blocks are at least partially escaped. Consequently, there cannot be a secondary transition. However, if $r_1 < 0.5$, then upon first escape the sticker block remains underneath the obstacle and the first block remains wholly confined. Thus, a second transition, associated with the escape of the first block, can occur at stronger compression. At smaller separations, the higher-order terms in $g(\tilde{H})$ come into play, giving rise to another drop in the free energy and the second escape transition. Very similar results occur for smaller obstacles; however, here the first escape transition occurs at larger separations such that successive terms in $g(\tilde{H})$ beyond the first term become important. For these smaller obstacles, the first transition occurs at $\tilde{H} \tilde{L} < 3.0$ and now depends slightly more upon the size of the first block. The behavior here is qualitatively similar to that seen for the exact solution of finite chains that is described in the next section.

3. Exact Solution for Finite Chains

In this section we construct an exact solution of the partition function which clearly shows the character of the multiple escape transitions. This exact calculation overcomes the inherent uncertainties associated with the approximate theory of the last section and with computer simulation.

3.1. Formalism of the Partition Function. As our aim is to construct an exact solution, we must consider a chain model for which the partition function and associated properties are analytically solvable and which describes the ideal block copolymer chain. For tractability of the partition function, a bonding potential between monomers i and $i + 1$ is chosen to be of the form^{13,17}

$$k(|x_{i+1} - x_i| + |y_{i+1} - y_i| + |z_{i+1} - z_i|) \quad (6)$$

where the coordinates of monomer i are given by (x_i, y_i, z_i) . A chain of N such monomers becomes Gaussian as N increases, and so the properties of the chain will become independent of the specific form of the bonding potential. The average separation, a , between bonded monomers in bulk solution is $a^2 = 6(k_B T / k)^2$; the average end-to-end distance is $a(N - 1)^{1/2}$; and the radius of gyration, R_g , is given by $R_g^2 = (N - 1/N)a^2/6$. This monomer–monomer potential has been previously used for force calculations in a slit¹⁷ and for the squashing of a nonadsorbing ideal polymer chain.¹³ The

interaction of each monomer with the obstacle surface is represented by a sticky potential.¹⁸ Monomer i is assumed to have some short-range adsorption potential $\psi_i(z)$ at a distance $z \geq 0$ from the obstacle surface, and the Boltzmann factor is written as $\exp(-\beta\psi_i(z)) \approx 1 + \bar{W}_i\delta(z)$, where $\delta(z)$ is a one-sided delta function, $\beta = 1/(k_B T)$, and \bar{W}_i is referred to as the adsorption strength of monomer i and is given by $\bar{W}_i = \int_0^\infty (\exp(-\beta\psi_i(z)) - 1) dz$. This representation of the adsorption strength should be adequate on length scales greater than the range of the adsorption potential. Since the adsorption strength can be varied independently for each monomer, this approach can be used to model multiblock copolymers, where the blocks of monomers are distinguished by their interaction with the surfaces. (Since the chain is ideal, the blocks do not interact with each other.)

We construct an analytic expression and solution for the partition function of such a chain, end-tethered and compressed between finite obstacles. The obstacle geometry, illustrated in Figure 1, is chosen to be two-dimensional in order to reduce the complexity of the analytic solution. The $i = 1$ monomer is fixed at the (x, z) origin, selected to be radially centered and midpoint between the two obstacles. The two impenetrable obstacles exclude monomers from the regions $|x| < L$, $z > H/2$ and $|x| < L$, $z < -H/2$, so that the compression distance or slit separation is H and the half-width of the obstacle is L . The partition function for the chain is then given by

$$Z(H) = \int_{A_2} \cdots \int_{A_N} \exp(-\beta k \sum_{i=1}^{N-1} (|x_{i+1} - x_i| + |z_{i+1} - z_i|)) f(x_p, z_p, \bar{W}_p, \bar{Y}_p) \prod_{i=2 \dots N} dz_i dx_i \quad (7)$$

where

$$\begin{aligned} f(x_p, z_p, \bar{W}_p, \bar{Y}_p) &= 1 + \bar{W}_p \left(\delta\left(z_i + \frac{H}{2}\right) + \delta\left(z_i - \frac{H}{2}\right) \right) \\ &\quad \text{for } |z_i| \leq H/2, |x_i| < L \\ &= 1 + \bar{Y}_p (\delta(x_i + L) + \delta(x_i - L)) \\ &\quad \text{for } |z_i| \geq H/2, |x_i| \geq L \\ &= 1 \quad \text{for } |z_i| \leq H/2, |x_i| > L \end{aligned}$$

A_i is the allowed area for monomer i , i.e., all area apart from $|x_i| < L$, $|z_i| > H/2$. We have distinguished two different adsorption strengths: the first, \bar{W}_i , is the adsorption strength of monomer i on the faces of the obstacles, and the second, \bar{Y}_i , is that on the sides of the obstacles. The solution procedure is very similar to that employed in an earlier paper¹³ and is summarized in the following sentences. As we proceed through the integrals in eq 7 and integrate out the coordinates of monomer i , we find that all of the resulting terms have a certain general form as functions of x_{i+1} and z_{i+1} , making it possible to derive recurrence relations for the coefficients of the terms. These coefficients can in turn be used to obtain an analytic expression for $Z(H)$ and its derived quantities such as compressive force, given by $f(H) = -1/Z \partial Z(H)/\partial H$. The details of this procedure and the resulting expressions are given in the Supporting Information.

One can now evaluate the partition function and its derivative with respect to H , as functions of H , L , a , \bar{W}_i , and \bar{Y}_i . A simple Fortran 90 code to perform this

evaluation is available from the authors. The main limitation of the numerical scheme is due to the finite precision of computer arithmetic. The region of most interest in the problem is for $H \ll R_g$, and as N increases, there is a growing loss of precision. In ordinary double-precision arithmetic, this limits N to about 50, depending somewhat on the value of L . This can be extended to around $N = 100$ using quadruple precision, but at the cost of a significant increase in computation time.

In the results that follow, we take all monomers in the adsorbing blocks to have the same adsorption strength while monomers in nonadsorbing blocks have $\bar{W}_i = 0$, and we restrict ourselves to the case where there is no difference between the adsorption on the two surfaces, i.e., $\bar{W}_i = \bar{Y}_i$. It is convenient to use a dimensionless adsorption strength given by $W_i = \beta k \bar{W}_i$. If for example the adsorption potential was a square well with width equal to the monomer–monomer spacing, then $W = 1$ corresponds to a well depth of $0.34 k_B T$ per monomer.

3.2. Exact Results from the Partition Function.

The formalism described above allows us to describe exactly the compressive force profiles of ideal block copolymers with a wide range of block arrangements. Our aim is to show that multiblock copolymers may exhibit multiple escape transitions whose number and critical compression depend on the arrangement of the adsorbing blocks along the contour of the chain, confirming the results of the approximate state model in the previous section. Thus, we limit our results to the following cases. First we consider the case of an adsorbing homopolymer and show the effect of the adsorption strength upon the escape transition. Then we focus upon polymers consisting of nonadsorbing blocks separated by short strongly adsorbing blocks or “stickers”, since these can give rise to multiple escape transitions. Note again that the stickers are laterally mobile on the surfaces of the obstacles. First a chain with one sticker is considered and then two stickers. The effect of varying the obstacle width is examined, and then, finally, some results are given for the root-mean-square displacement of the free end of the chain as the polymer is compressed.

Figure 4 shows the force profiles for $N = 40$ homopolymers with a dimensionless adsorption strength W ranging from 0 (nonadsorbing) to 1.2 when compressed between cylinders of size $\bar{L} = 3.0$. For a nonadsorbing homopolymer, the escape transition is marked by a maximum/minimum or an inflection at $\bar{H} \approx 0.55$. With larger adsorption strengths or more attractive monomers, the escape transition occurs at smaller separations and eventually disappears as the monomers are made highly adsorbing. This occurs as the energy gained through adsorption onto the two opposing faces of the cylinders outweighs the confinement penalty and is more favorable than chain stretching and adsorption on the exterior surfaces of the cylinders. In a slit of finite width the force profile for the ideal chain with $W = 1$ is very weakly attractive, as seen in Figure 4, and for more adsorbing polymers the force becomes strongly attractive at all separations. The critical adsorption strength, above which a model polymer of this kind adsorbs strongly to the surface, is $\bar{W} = 1$. In an infinite slit, the ideal polymer with this adsorption strength gives a net force of zero, since the adsorption exactly balances the restrictive entropic effect of the walls.¹⁷ This is an

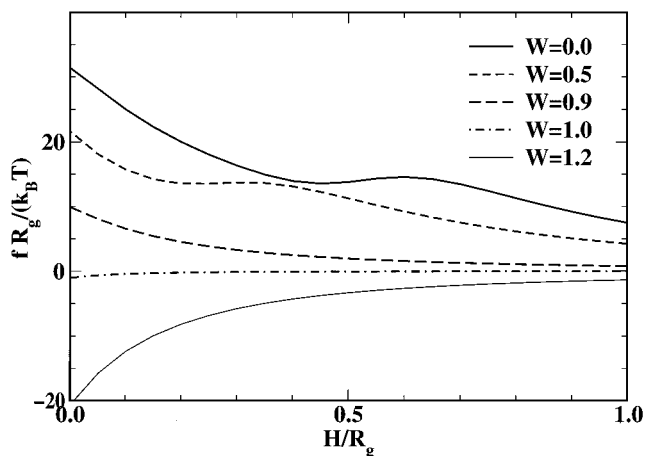


Figure 4. Dimensionless force, $fR_g/(k_B T)$, vs dimensionless compression distance, \bar{H} , for an adsorbing homopolymer of $N = 40$ monomers between obstacles of half-width $\bar{L} = 3$. The results, obtained from a rigorous numerical evaluation of the partition function, are plotted for different values of the dimensionless adsorption strength, ranging from $W = 0$, corresponding to an inert nonadsorbing homopolymer, to $W = 1.2$, where adsorption is so favorable that the obstacles are weakly attractive.

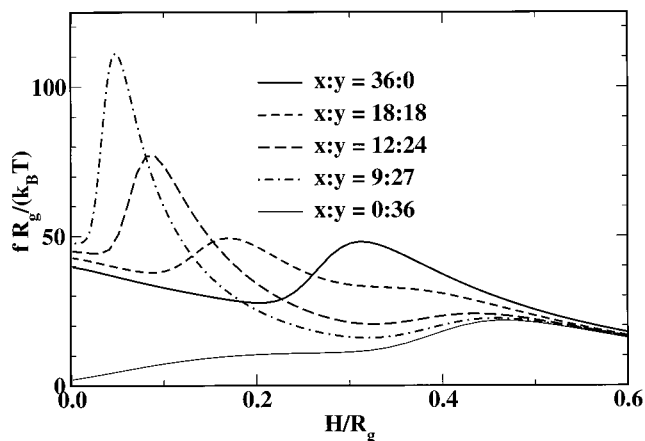


Figure 5. Dimensionless force, $fR_g/(k_B T)$, vs dimensionless compression distance, \bar{H} , for a $N = 40$ block copolymer which has one sticker block and is compressed between obstacles of half-width $\bar{L} = 4$. The block copolymer has one adsorbing sticker block of four monomers, each with adsorption strength $W = 10$, and separates two nonadsorbing blocks. The results are plotted for several different positions of the sticker block. The position of the sticker block is specified as $x:y$, where x is the number of nonadsorbing monomers in the first nonadsorbing block (positioned at the tethering point) and y is the number of monomers in the nonadsorbing block positioned at the free end of the polymer chain.

artifact of an ideal chain model that does not account for any monomer–monomer interactions. Even in Θ solvent conditions there are higher-order excluded-volume effects which give rise to a repulsion at very short separations as the density of the polymer increases sufficiently.¹⁹

Now consider a tethered polymer that has one short strongly adsorbing block of monomers which is inserted along the chain contour. Depending upon where this sticker is located along the chain contour, we expect different signatures in the force profiles. Figure 5 shows the force profiles for chains of $N = 40$ monomers that contain a sticker block of four monomers, each with $W = 10$, at different positions along the chain contour. The ordering of the blocks is indicated by the ratio $x:y$ where,

starting from the tethered end, there are x nonadsorbing monomers followed by the sticker block which is followed by y nonadsorbing monomers that form the free end or “tail” of the chain. When the sticker block is located at the free end of the chain, then the chain is a simple loop of nonadsorbing monomers with its free end adsorbed onto one of the cylinder surfaces and (following the notation of the previous section) $r_1 = 1$. For a single loop, there is at most a single escape transition which occurs at a stronger compression (smaller \bar{H}) than that of a simple end-tethered polymer. Indeed, this is confirmed by the partition function calculations of Figure 5 which show the force profile of the looplike copolymer, labeled $x:y \equiv 36:0$, and the profile of the free-tail-like copolymer, labeled $x:y \equiv 0:36$. Although a “critical compression” is difficult to extract from these maximum–minimum traces, taking the inflection point as characteristic of the first escape transition shows that the chain having the free end escapes more easily (at weaker compression) than the loop. Note that for the $x:y \equiv 0:36$ profile the compressive force continues to decrease after escape of the free end or tail; this is due to the bridging of the short sticker block between the opposing cylinder faces.

If we shift the sticker block from the tethered end toward the free end, we are effectively increasing the size of the loop or the first block at the expense of the second nonadsorbing block that forms the free tail. When this loop is very small and the tail is large, for example $r_1 = 0.25$ or $x:y \equiv 9:27$, then the tail first escapes at roughly the same compression as a full tail (i.e., $x:y \equiv 0:36$), but it takes a severe compression to cause the escape of the small loop. Indeed, the escape of the loop, i.e., the second escape, is much easier to detect in these theoretical force profiles due to the high maximum force required at such small separations. As the sticker is shifted to make the first block or loop bigger and the second block or tail smaller, the second escape becomes easier (i.e., smaller forces and weaker compression). However, as the tail becomes small (say toward 0 as in $x:y \equiv 36:0$), the tail fully escapes with the partial escape of the loop. That is, there is only one escape transition. It is important to recognize that the ordering of the blocks along the chain contour is significant, since the free end escapes first. A chain with architecture $x:y \equiv 12:24$ has quite a different force profile to one with blocks $x:y \equiv 24:12$. Thus, the number and location of the escape transitions provide some information about the structure of the compressed polymer.

In the above example, it was shown that a polymer with two nonadsorbing blocks can have a force profile with two escape transitions. So the question arises as to whether a polymer with a more complex architecture can give rise to more than two escape transitions. Consider a chain with $N = 44$ monomers and two sticky blocks, each of length four monomers with an adsorption strength of $W = 10$. These two sticky blocks partition the chain into three nonadsorbing blocks, and the arrangement of these blocks is labeled $x:y:z$ where x is the number of nonadsorbing monomers in the block closest to the tether end and z is that at the free end of the chain. Figure 6 shows the predicted force profiles for some possible multiblock arrangements. If the nonadsorbing blocks are of equal size ($x:y:z \equiv 12:12:12$), then two distinct escape transitions are observed. The one at larger separation corresponds to the escape of the two

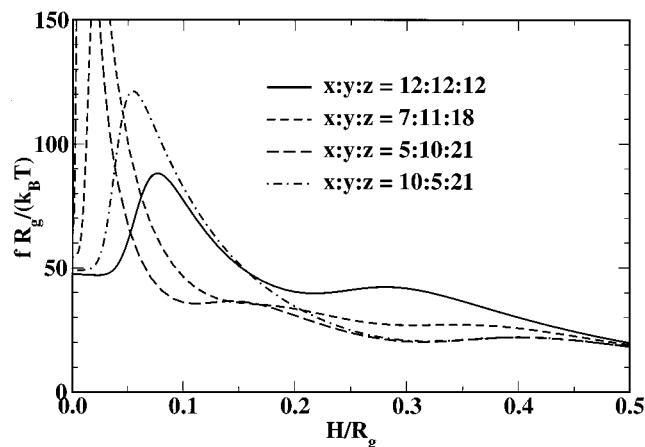


Figure 6. Dimensionless force, $fR_g/(k_B T)$, vs dimensionless compression distance, H , for a $N = 44$ block copolymer which has two sticker blocks and is compressed between obstacles of half-width $\tilde{L} = 4$. The block copolymer has two adsorbing sticker blocks of four monomers, each with adsorption strength $W = 10$ which separate three nonadsorbing blocks. The results are plotted for several different positions of the sticker blocks. The position of the sticker blocks is specified as $x:y:z$, where x is the number of nonadsorbing monomers in the first nonadsorbing block (positioned at the tethering point), y is the number of monomers in the middle nonadsorbing block, and z is the number of monomers in the nonadsorbing block positioned at the free end of the polymer chain. However, depending upon the size of the chain, these compression distances may be on the order of a monomer size where the compressive force is experimentally inaccessible and questions regarding the model cloud the interpretation.

nonadsorbing blocks at the end (or at least the escapes of these two blocks are too close together to yield distinct local maxima in the force curve), and a second escape transition at smaller separation corresponds to the escape of the nonadsorbing block nearest the tethering point. As the sizes of the nonadsorbing blocks are made more disparate (e.g., $x:y:z \equiv 7:11:18$), further structure appears in the force curve, until for the architecture $x:y:z \equiv 5:10:21$, three distinct escape transitions are observed, corresponding to the successive, individual escapes of the three nonadsorbing blocks. If the order of the blocks in the last case is changed to $10:5:21$, then the first transition is the same, but there is only one other escape transition. Once the outermost nonadsorbing block has escaped, then the compression of the remaining part of the polymer between the obstacles is similar to the examples in Figure 5 for a single sticky block, which indicated that two further transitions are only possible for increasing block sizes. These numerical predictions and the more qualitative, coarse-grained description of the previous section provide the following simple observation. An ideal polymer with m distinct nonadsorbing blocks will most likely exhibit m escape transitions if the ratio of block sizes increases in some geometric progression as one moves along the chain contour from the tethered end to the free end.

Does the structure of the force profile change as the size of the compressing cylinders, \tilde{L} , is varied? Figure 7 shows the force profiles for a $N = 44$ copolymer with block arrangement $x:y:z \equiv 5:10:21$ compressed between cylinders of radii $\tilde{L} = 0.1, 1, 3,$ and 5 . This shows that as we progressively increase the cylinder radii, we see additional transitions. When the cylinders are smaller than the radius of gyration of the copolymer, no escape transition is observed; in fact, the force is monotonically

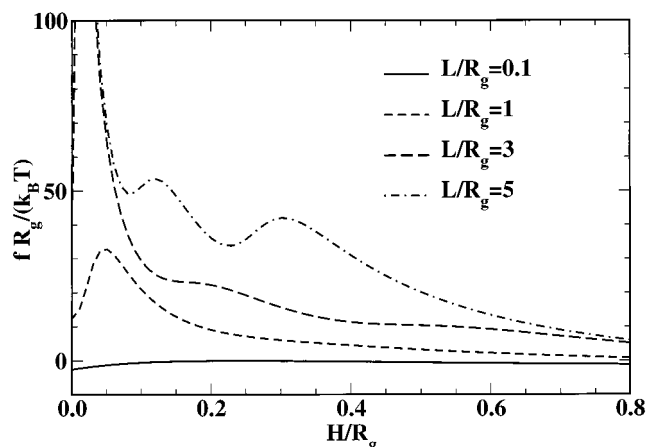


Figure 7. Dimensionless force, $fR_g/(k_B T)$, vs dimensionless compression distance, H , for a $N = 44$ block copolymer which has two sticker blocks with positioning $x:y:z = 5:10:21$ and is compressed between obstacles of various half-width, ranging from $\tilde{L} = 0.1$ to $\tilde{L} = 5$. The block copolymer has two adsorbing sticker block of four monomers, each with adsorption strength $W = 10$ which separate three nonadsorbing blocks. Note that as the obstacle size increases, the maxima/minima in the compressive force profile associated with the three escape transitions become more pronounced.

attractive. At $\tilde{L} = 1$ compression leads to a single transition at very small separations. At $\tilde{L} = 3$, this transition at very small separations is retained, albeit shifted to yet smaller separations and at higher compressive force. But there is also another transition that appears at weaker compression (larger separation). Finally, at $\tilde{L} = 5$ yet another transition occurs at even weaker compression.

The effect of chain architecture on the escape transition can be further understood by examining the root-mean-square displacement of the monomers on the free end of the chain in the z direction (the "vertical" direction, along the axis of the two obstacles) as a function of compression and for different values of L/R_g . This is shown in Figure 8 for a $5:10:21$ copolymer and the same set of cylinder radii as in Figure 7. When the obstacles are much smaller than the radius of gyration of the first nonadsorbing block (e.g., the solid curve for $L/R_g = 0.1$), the sticker blocks are largely adsorbed on the outside surfaces of the obstacles as much of the chain has already escaped. Thus, as the separation decreases and the cylinders are displaced toward each other, the relative height of the free end from the tethered end (i.e., the z distance) decreases. When L/R_g is larger and the chain is initially confined, there is first a compression of the polymer chain in the vertical z direction, and then as it begins to escape, the free end can move out from underneath the obstacle and up in the vertical direction. For this multiblock chain, at larger values of L/R_g the vertical z displacement vs separation curve begins to show additional structure, with steps corresponding to the escape of the next nonadsorbing block along the chain, which allows the free end to explore further in the vertical direction. Thus, the displacement of the chain end in the vertical direction as a function of separation also gives information on the chain architecture and confirms the interpretation of the successive escape transitions.

4. Discussion

Here we have used two different theoretical approaches to study the compression under a finite

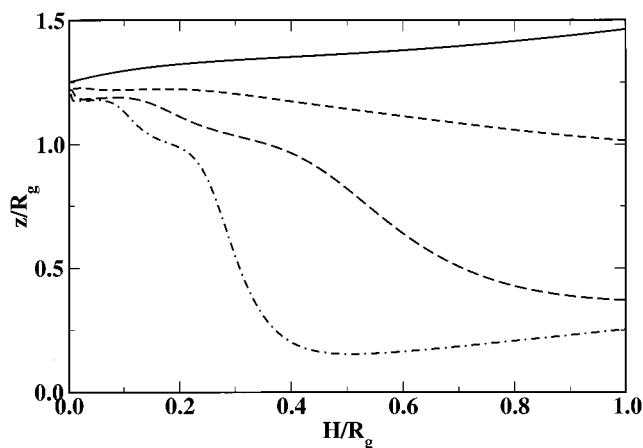


Figure 8. Root-mean-square displacement of the end of the chain in the perpendicular z direction, z/R_g , vs dimensionless compression distance, \bar{H} , for the same polymer architecture as in Figure 7 (i.e., a $N = 44$ block copolymer which has two sticker blocks of length four monomers, each with $W = 10$, and the other monomers are nonadsorbing. The sizes of the nonadsorbing blocks are 5, 10, and 21 monomers, respectively, as one moves along the chain away from the tethering point). The polymer is compressed between obstacles of various half-width, ranging from $\bar{L} = 0.1$ to $\bar{L} = 5.0$ (curves as in Figure 7).

obstacle of an end-grafted ideal copolymer comprised of alternating adsorbing and nonadsorbing blocks. Both techniques show that the size and ordering of the blocks determine the number of escape transitions and the critical compressions at which they occur. Such escape transitions are marked by a discontinuous exchange of monomers from the confined slit to outside of the obstacles and a decrease in the compressive force. The first approach is an approximate solution for long chains having large nonadsorbing blocks separated by short, strongly adsorbing blocks. The procedure is to estimate the Helmholtz free energy of the chain in various states, each state corresponding to the partial escape of successive nonadsorbing blocks. From these state energies we can express the state of the chain as being that with the minimal free energy, or alternatively we can construct an approximate partition function from these discrete states. This solution is simple and provides a simple physical picture, but it is not obvious how the approximations involved affect the quantitative predictions. The second approach that we adopted is a solution of the exact partition function for model chains of finite length where monomers are assigned specific adsorption strengths depending upon the block in which they reside. This solution has the advantages that it is exact and therefore provides unambiguous results. However, due to computational constraints, we are limited to relatively short chains so that limited comparison can be made with the long chain approximate solution.

The qualitative behavior predicted by the two approaches is broadly similar. For a nonadsorbing homopolymer, when the dimensionless separation $\bar{H} = H/R_g$ is such that $\bar{H}\bar{L} \approx 3$ (where $\bar{L} = L/R_g$ is the size of the obstacle and R_g is the radius of gyration of the polymer), then the outer half of the chain escapes from between the obstacles, giving rise to a local maximum in the force vs separation curve. If the homopolymer is made uniformly adsorbing, then the escape transition moves to smaller separations and disappears entirely above a critical adsorption strength. For a chain composed of m nonadsorbing blocks separated by short

stickers, there can be up to m escape transitions upon compression, depending upon the obstacle size and the ratios of block sizes. The maximum number of transitions is generally seen when $\bar{L} \gg 1$, and the sizes of the nonadsorbing blocks increase along the chain away from the tethering point.

We have shown theoretical predictions using a range of compressions, including very high compressions or \bar{H} approaching 0. Depending upon the size of the chain, these compression distances, \bar{H} , may be on the order of a monomer size, a , where the compressive force is experimentally inaccessible and questions regarding the model cloud the interpretation. As \bar{H} approaches the (statistical) monomer length scale (< 10 nm), the roughness of the AFM tip and surface forces may mask any forces attributable to the chain and its conformation. On the theoretical side, the energy formalism used in the approximate state model is only appropriate when $\bar{H} \gg a$. In addition, the spring potential used in the exact partition function evaluation allows predictions that correspond to the squeezing out of all monomers (other than the anchoring one) out of the slit. That is, it predicts a finite compressive force as \bar{H} tends to 0. Thus, care is needed in interpreting our results when \bar{H} tends to 0.

Finally, it is also important to recognize that all of our results correspond to chains continually in equilibrium at any compression. This is an important point as the activation energy between the confined and (first) escaped state, corresponding to the energy of stretching a chain to the edge of the obstacle, can be appreciable, i.e., many $k_B T$. The activation energy between the first escaped state and a secondary escape state (or between two secondary escape states) is associated with the "extra" stretching that the chain must accomplish for the secondary escape without significant relief of confinement of nonadsorbing monomers. Thus, we anticipate that the activation energy for subsequent escape transitions should increase with the size of the outermost, confined adsorbing block.

Supporting Information Available: An appendix giving the equations for the exact solution of the discrete chain between two finite obstacles. This material is available free of charge via the Internet at <http://pubs.acs.org>.

References and Notes

- (1) de Gennes, P. G. *Scaling Concepts in Polymer Physics*; Cornell University Press: Ithaca, NY, 1979.
- (2) Doi, M.; Edwards, S. F. *The Theory of Polymer Dynamics*; Clarendon Press: New York, 1986.
- (3) Subramanian, G.; Williams, D. R. M.; Pincus, P. A. *Europhys. Lett.* **1995**, *29*, 285–290.
- (4) Subramanian, G.; Williams, D. R. M.; Pincus, P. A. *Macromolecules* **1996**, *29*, 4045–4050.
- (5) Williams, D. R. M.; Mackintosh, F. C. *J. Phys. II* **1995**, *5*, 1407–1417.
- (6) Guffond, M. C.; Williams, D. R. M.; Sevick, E. M. *Langmuir* **1997**, *13*, 5691–5696.
- (7) Jimenez, J.; Rajagopalan, R. *Langmuir* **1998**, *14*, 2598–2601.
- (8) Jimenez, J.; Rajagopalan, R. *Eur. Phys. J. B* **1998**, *5*, 237–243.
- (9) Artega, G. A. *Int. J. Quantum Chem.* **1997**, *65*, 519–530.
- (10) Milchev, A.; Yamakov, V.; Binder, K. *Phys. Chem. Chem. Phys.* **1999**, *1*, 2083–2091.
- (11) Milchev, A.; Yamakov, V.; Binder, K. *Europhys. Lett.* **1999**, *47*, 675–680.
- (12) Sevick, E. M.; Williams, D. R. M. *Macromolecules* **1999**, *32*, 6841–6846.
- (13) Ennis, J.; Sevick, E. M.; Williams, D. R. M. *Phys. Rev. E* **1999**, *60*, 6909–6918.
- (14) Sevick, E. M. *Macromolecules* **2000**, *33*, 5743–5746.

- (15) Grosberg, A. Y.; Khokhlov, A. R. *Statistical Physics of Macromolecules*; AIP Press: New York, 1994.
- (16) Dolan, A. K.; Edwards, S. F. *Proc. R. Soc. London A* **1974**, *337*, 509–516.
- (17) Ennis, J.; Jönsson, B. *J. Phys. Chem. B* **1999**, *103*, 2248–2255.
- (18) Chan, D.; Mitchell, D. J.; Ninham, B. W.; White, L. R. *J. Chem. Soc., Faraday Trans. 2* **1975**, *71*, 235–268.
- (19) Ingersent, K.; Klein, J.; Pincus, P. *Macromolecules* **1990**, *23*, 548–560.

MA0008802